HHS Public Access

Author manuscript

Neuroscience. Author manuscript; available in PMC 2015 April 17.

Published in final edited form as:

Neuroscience. 2012 August 2; 216: 57–69. doi:10.1016/j.neuroscience.2012.04.062.

Interactions between two propagating waves in rat visual cortex

Xin Gao[1,2,3], **Weifeng Xu**[3], **Zhijie Wang**[1,2], **Kentaroh Takagaki**[4,5], **Bing Li**[1,*], and **Jian-young Wu**[3,*]

[1]State Key Laboratory of Brain and Cognitive Science, Institute of Biophysics, Chinese Academy of Sciences, Beijing 100101, China

[2]Graduate University of Chinese Academy of Sciences, Beijing 100049, China

[3]Department of Neuroscience, Georgetown University Medical Center, Washington, DC 20057, USA

[4]Georgetown University Hospital, Washington, D. C., 20007 USA

[5]Leibniz Institute for Neurobiology, Magdeburg, 39118 Germany

Abstract

Sensory-evoked propagating waves are frequently observed in sensory cortex. However, it is largely unknown how an evoked propagating wave affects the activity evoked by subsequent sensory inputs, or how two propagating waves interact when evoked by simultaneous sensory inputs. Using voltage-sensitive dye imaging, we investigated the interactions between two evoked waves in rat visual cortex, and the spatiotemporal patterns of depolarization in the neuronal population due to wave-to-wave interactions. We have found that visually-evoked propagating waves have a refractory period of about 300 ms, within which the response to a subsequent visual stimulus is suppressed. Simultaneous presentation of two visual stimuli at different locations can evoke two waves propagating toward each other, and these two waves fuse. Fusion significantly shortens the latency and half-width of the response, leading to changes in the spatial profile of evoked population activity. The visually-evoked propagating wave may also be suppressed by a preceding spontaneous wave. The refractory period following a propagating wave and the fusion between two waves may contribute to visual sensory processing by modifying the spatiotemporal profile of population neuronal activity evoked by sensory events.

Keywords

propagating wave; voltage-sensitive dye imaging; refractory period; fusion

*Correspondence to:Jian-young Wu wuj@georgetown.edu, Address: Basic Science Building Room 207A, 3900 Reservoir Road, NW, Washington, DC 20057, USA, Phone: +1 202 687 1614 Or Bing Li lib@sun5.ibp.ac.cn, Address: 15 Datun Road, Chaoyang District, Beijing, 100101, China.

Introduction

Propagating waves of neuronal activity are frequently found when a large number of cortical neurons are activated by sensory events (London et al., 1989; Prechtl et al., 1997; Senseman and Robbins, 1999; Prechtl et al., 2000; Jancke et al., 2004a; Ferezou et al., 2006; Roland et al., 2006; Song et al., 2006; Benucci et al., 2007; Ferezou et al., 2007; Sharon et al., 2007; Xu et al., 2007; Takagaki et al., 2008b; for reviews, see Ermentrout and Kleinfeld, 2001; Wu et al., 2008; Wang, 2010). A single visual object presented in the visual field induces a propagating wave in the primary visual cortex (V1), starting spatially from the retinotopic site of the visual stimulus (Bringuier et al., 1999; Roland et al., 2006; Xu et al., 2007; Han et al., 2008). During natural vision, when multiple objects are seen in the visual field simultaneously or sequentially, multiple waves may be initiated and interact. The interaction between these waves may play important roles in cortical visual processing.

Such interactions between propagating waves are frequently observed in the cortex, and particularly well described in the barrel cortex. For example, spontaneous sleep-like waves can suppress a wave evoked by whisker stimulation (Petersen et al., 2003b). Cortical activities evoked by whisker deflection can suppress the amplitude and spatial area of a subsequent evoked response (Civillico and Contreras, 2006). Furthermore, interactions between two spontaneous waves may initiate spiral waves and other complex spatiotemporal patterns (Huang et al., 2004; Schiff et al., 2007; Huang et al., 2010b). Despite the frequent observation of wave interactions, many questions remain on how cortical propagating waves interact. For example, given that the population undergoes only subthreshold depolarization during a wave, when two waves collide, does the average population depolarization increase? What happens when one wave runs into the tail of another wave? Furthermore, are there any changes in the population response at different locations due to wave-to-wave interaction? What is the spatiotemporal distribution of these changes? This report will study wave-to-wave interactions in rat visual cortex by simultaneously or sequentially presenting two small visual objects in the visual field.

Voltage-sensitive dye (VSD) signals from the cortex correlate well with membrane potential changes at the population level (for reviews, see Grinvald and Hildesheim, 2004; Huang et al., 2010a). This allows examination of population depolarizations and hyperpolarizations during a cortical event. In this report, we demonstrate that a visually-evoked wave can suppress subsequent waves evoked by another visual object, within a time window of 80 to 300 ms. Two simultaneous waves evoked at different locations can fuse when the wave fronts meet. The fusion changes the latency and half-width of the evoked response, as well as the propagation direction of the wavefront, depending on the spatiotemporal relationship of wave initiation sites and timing. The VSD signals do not sum when two waves fuse, suggesting that the fusion of the waves does not increase the level of depolarization in the population.

Methods

Surgical procedures

Sprague-Dawley rats (250 – 400 g, n = 26) and Long Evans rats (250 - 350g, n = 35) were used in the experiments. Surgical procedures were approved by the institutional Animal Care and Use Committee of Georgetown University following the guidelines of the National Institutes of Health.

Animals were pretreated with a dexamethasone sulfate (1 mg/kg) by intraperitoneal (IP) injection one night before and an IP injection of atropine sulfate (60μg/kg) approximately 30 minutes before the surgery. Anesthesia was induced with ketamine (60mg/kg) and xylazine (15mg/kg). After tracheostomy, the animals were ventilated with a small animal respirator delivering 1.5-2% isoflurane in oxygen or room air. The respiratory rate (60-100 c/min) and volume (2-3 ml) were adjusted such that the end-tidal CO_2 was 26 - 32 mmHg (3.3 - 4.2 %). The body temperature of the anesthetized animals was maintained at 37°C with a regulated heating pad. In some experiments, 4% isoflurane was used to induce the anesthesia. Urethane (1g /kg) was injected (IP) after tracheostomy and isoflurane was reduced to 1.5% for surgery. The animal was fixed by ear bars on a stereotaxic apparatus. A cranial window (5×5 mm^2) was drilled over the visual cortex of the left hemisphere (bregma -4 to -9 mm, lateral 2- 7 mm). A Vaseline chamber was made on the bone around the window.

Dye staining

Voltage-sensitive dyes RH1838 or RH1691 (Optical imaging) were used to stain the cortex (1mg/ml, in Ringer's solution). The dura was removed. After staining for 90 min, the cortex was washed with dye-free ringer solution for approximately 30 minutes. In some experiments, the cortex was stained through the dura. In order to increase dural permeability to the dye, we dried the dura with gentle air flow before staining. During staining, the dye solution was continuously circulated by a perfusion pump.

Optical imaging

High viscosity silicone oil (30,000 centistokes) was applied to the surface of the cortex, and the chamber was sealed with a glass coverslip. Voltage-sensitive dye imaging experiments were performed in two apparatuses: the apparatus at the Institute of Biophysics in Beijing, China uses a 150W Xenon arc lamp (Opti Quip) as light source, the light was filtered by a Chroma Cy5 filter cube (Chroma) with 640±20 nm excitation filter, 660 nm dichroic mirror and 680 ±30 nm emission filter. Data for Figures 1 - 4 were mainly collected using this apparatus. The apparatus at Georgetown University uses a 100 W Tungsten halogen lamp (Zeiss) and the light was filtered by a custom filter cube (Chroma) with 630±30 nm excitation filter, 660 nm dichroic mirror and 690 ±30 nm emission filter. Data for Figures 5 -6 were collected using this apparatus. The latter apparatus has higher light throughput and also better signal-to-noise ratio. In both apparatuses, the dye fluorescence light was collected by a 5x macroscope modified from a Navita 25 mm f = 0.9 video lens. The real image of the cortex was projected onto the aperture of a 464-channel photodiode array (WuTech Instruments). Each channel (photodiode) of the array receives light from a cortical area of 160 μm in diameter. Most of the signal comes from cortical layers II-III (Lippert et al.

2007). A two-stage of amplification in the diode array produces an effective 19 bits of dynamic range, adequate to detect 0.01% dF/F signals. The optical signals were digitized at 1.6 KHz by an A/D converter (Microstar Labs) with a desktop computer. Local EEG was recorded with a silver ball electrode placed at the edge of the cranial window. The EEG signals were filtered between 1 Hz to 100 Hz and amplified 1000 times. ECG of the animal was also collected and digitized simultaneously with the optical and EEG signals. ECG was used to trigger a custom algorithm for removing heartbeat artifact from optical signals (Lippert et al., 2007). Data were acquired with NeuroPlex software (RedShirtImaging, Detacur, GA). All data were collected as single trials. Each imaging trial lasted for 3 s with an inter-trial interval of >100 s. For additional information regarding the diode array and VSD methods see Wu and Cohen (1993), Jin et al. (2002), Lippert et al. (2007) and Huang et al. (2010a).

Visual stimulation

Visual stimuli were generated by programs written in Visual C++. The patterns were displayed on a CRT or LCD (70°h × 55°w in visual angle, 800 × 600, 85Hz) placed in front of the eye contralateral to the imaged visual cortex. The visual stimulus consisted of one or two bright squares (80 cd/m^2) on black background (3 cd/m^2 or below) occupying 10 degrees of visual space, with a duration of 100 ms.

At the beginning of each experiment, the imaging field was adjusted so that a large part of area V1 and the initiation site of the evoked responses were within the imaging field.

Electrical stimulation

Electrical stimuli consisted of single pulses (0.1 ms duration), with intensities of 10~25 μA (2~5 V), delivered to the surface layer of visual cortex through a tungsten electrode (200 kΩ). The stimulation site was placed near the posterior edge of the imaging window. The reference electrode was placed on tissue outside the skull next to the cranial window.

Data analysis and presentation

The optical data were analyzed in NeuroPlex and scripts written with Matlab (Mathworks). Raw data were first processed by a custom algorithm written in Matlab to remove heartbeat artifacts (Lippert et al., 2007), then filtered digitally before presentation as traces (e.g., Figure 1C) or pseudo-color images. The pseudo-color images (excluding Figure 2) were generated from fractional changes of the fluorescent light in each trial, and were smoothed with a 3 × 3 mean spatial filter. The signal on each detector was individually scaled to occupy the full range of the color map (Grinvald et al., 1982; Jin et al., 2002; Lippert et al., 2007).

Definition of the wave latency and half-width

At a given detector, the latency of the response was defined as the lag of the peak response from the stimulus onset (Figure 2A). The half-width was defined as the lag between the responses reaches 50% of the peak and the peak (Figure 2A).

Results

Various interactions between two visually-evoked waves

Visually-evoked cortical activity manifests as propagating waves, starting from the retinotopic site of stimulation in the visual field (Roland et al., 2006; Benucci et al., 2007; Xu et al., 2007; Han et al., 2008). Sequentially displaying two visual stimuli (Figure 1A) evokes two propagating waves interacting within the primary visual cortex (V1) of the left hemisphere (Figure 1). Since the location and timing of the visual stimuli on the screen determined the initiation site and onset time of the propagating waves, we could accurately control the location and timing of the interacting waves. By changing the inter-stimulus interval (ISI) of the two stimuli, we studied the interaction of these waves with each other.

In the experiment shown in Figure 1, the visual stimulus was presented at the bottom or top of the visual field and evoked a propagating wave from anterior or posterior retinotopic locations in the V1 (Figure 1B right images). Evoked activity propagated at 0.065 ± 0.019 (mean ± SD) m/s in the rostral-caudal direction (N = 25 animals, averaging done after calculation of propagation speed in each trial). When the two stimuli were presented sequentially, e.g. bottom square (St1) followed by the upper square (St2), the two evoked waves interacted in V1 as observed in optical traces (Figure 1C left) and pseudo-color images (Figure 1C right). At an ISI of 300 ms or longer, the responses showed no apparent interactions, with the amplitude of the second evoked activity similar to that of the first (Figure 1C left, top two traces). The activity evoked by the second visual stimulus was not affected, because spatially, it initiated long after the first evoked wave propagated through the entire V1 area (Figure 1C right, top row images). Interactions occurred when the ISI was reduced. When the ISI was reduced to 160 ms, response to St2 was largely suppressed at a distant location (Figure 1, location 1) while less affected at the retinotopic site (Figure 1C, location 2). As shown by the pseudo-color images, the whole area was affected by the propagation of the first wave so that the second stimulus failed to evoke a full-scale propagating wave; only a local response was seen near the retinotopic site (Figure 1C right, middle row images). At an ISI of 30 ms, both traces showed one response peak (Figure 1C left, bottom two traces). The response to the second stimulus developed before the wavefront of the first response arrived at detector 2, so the two stimuli both evoked responses near their retinotopic sites and the activity fused as the propagating waves met (Figure 1C right, bottom row images). The amplitude of the VSD signal did not increase when the fusion occurred (Figure 1C left, bottom two traces), indicating that the fusion of two waves does not add to the extent of population depolarization.

The relationship between the ISI and the amplitude of the evoked waves is summarized in Figure 1D. At an ISI of 300 ms or longer, the amplitude of the second evoked response was not affected by the first wave (Figure 1D, marked by the orange bar). For ISIs between 80 and 300 ms, the amplitude of the second response was significantly reduced (Figure 1D, marked by the blue bar), indicating that the refractory period of an evoked wave is about 300 ms, during which the development of subsequent waves are suppressed. For ISIs between 0 and 30 ms, the response to St2 was unaffected at the retinotopic site and later fused with the wave evoked by the first stimulus (Figure 1D, marked by the red bar). We did not measure

amplitudes of the waves during ISIs of 30 to 80 ms, because the second evoked response and the approaching first wave were indistinguishable near detector 2 at these intervals. For repetitive stimulus at the same retinotopic location, the response to the second stimulus is also suppressed at the interval of 80-300 ms, similar to that of two point stimulus (data not shown).

Wave-to-wave interactions including fusion and suppression have large effects on population activity, spatially and temporally, which are described in the following section.

Fusion of two evoked waves

When two visually-evoked waves were initiated with a short ISI, we observed a significant reduction of the latency (as defined in Methods) over a large cortical area (Figure 2). Shortening of the latency was seen clearly in the optical signals, in single trials. In Figure 2B, we show optical signals from four representative detectors, two from the retinotopic sites (*i1, i2*), and two in the middle area between *i1* and *i2* (*M* and *P*, locations shown in Figure 2A). When stimulus St1 or St2 was given alone, the evoked wave manifested at these four detectors with timing determined by the wave propagation velocity. Thus, the latency was shortest at the initiation sites (*i1* for St1, *i2* for St2) and longer at the distant sites (*i2* for St1, *i1* for St2) (Figure 2B, *i1, i2*, blue and green traces). The middle points *M* and *P* were chosen to have similar distances to *i1* and *i2* so that the latency difference between the St1 and St2 evoked response was small (Figure 2B, *M, P*, blue and green traces). When St1 and St2 were given together with a short ISI of 15 ms, we observed marked latency shortening in the two middle detectors (Figure 2B red traces). This latency shortening was observed in all fifteen animals examined.

In the same animal, when the intensity and location of the stimuli were identical, the shortening of the latency was consistent from trial to trial, as in the example shown in Figure 2C (average result from 5 trials in the same preparation). The shortening of the latency was significant at middle points M and P within V1, and insignificant at the retinotopic initiation sites *i1* and *i2* (Figure 2C, comparing red and blue bars at *i1* and red and green bars of *i2*). This suggests that latency shortening is more obvious in those areas where waves fuse.

To better investigate the spatial profile of the latency change, we plotted this latency change throughout the whole imaging field. As shown in figure 2D, shortening of the latency occurs mostly in the middle area between two initiation sites, where the latency shortening can be as large as 25 ms. The latency change was small close to retinotopic sites. This distinct spatial profile suggests that outside retinotopic sites, activity is triggered primarily by the propagating wave, and thus wave fusion had a large impact. In contrast, sensory-evoked cortical activity is dominant near the retinotopic sites, and peaks earlier such that the wave fusion caused smaller latency changes here.

The fusion of the two evoked waves also reduced the half-width of the waveform, as seen both in the individual recording traces (Figure 2B, red and blue/green traces) and in grouped data (Figure 2E, left). Reduction of the wave half-width suggests that the two evoked waves act synergistically to accelerate depolarization onset. Despite large changes in the latency and half-width, the fusion of two waves caused no significant change in the response

amplitude, even at the middle detector where latency change was maximal (Figure 2E, right).

The fusion of the two evoked waves also changed the direction of the wave front. When stimulus St1 or St2 were given individually, the evoked wave propagated within V1 with an arched wavefront (Figure 3A, top two rows). In contrast, when St1 and St2 were presented simultaneously, the waves fused at the midpoint and propagated laterally from there (Figure 3A, bottom row, image marked by asterisks). The wave front contour lines drawn in Figure 3B show that the wave directional vectors point outward from the respective retinotopic sites when St1 or St2 is given alone (Figure 3B, blue and green arrows). Fusion between two waves changed the directional vector, such that the direction ran parallel to the midline between the two initiation sites (Figure 3B, red arrows). Changes in the propagating direction can also be seen in the space-time maps (X-T maps) (Figure 3C), which show that the signal from one column of optical detectors approximately parallel to the simultaneous wave front (the location of the detectors marked by gray box in Figure 3B). The depolarization along this column of optical detectors occurred nearly simultaneously when two visual stimuli were given at the same time (Figure 3C, bottom), markedly different from the activation when individual visual stimuli were given alone (Figure 3C, Top two). Similar changes in wave front were observed in all 15 animals in which we observed wave fusion.

Suppression of the second wave

As described in Figure 1D, the propagating wave evoked by the first visual stimulus (St1) suppressed the response to the second stimulus (St2) for ISIs of 80 to 300 ms. The suppression peaked for ISIs of ~100 ms, at which the response to the second stimulus was not detectable in more than 90% of the trials. Increasing the ISI increased the probability of the second stimulus evoking a population response. For ISIs between 200 and 300 ms, the second response was completely suppressed in about 15% of the trials, and only partially suppressed in the majority of other recording trials (Figure 4). Partial suppression appears to be more complex than complete suppression. The partially suppressed response can be dissected into two components, a local response followed by a delayed propagating wave. Both components are evoked by the second stimulus, but the local response is initiated on the retinotopic site, accurately associated with the stimulation timing and does not propagate (Figure 4B, right). In contrast, the delayed wave is a propagating event, initiated near but not exactly at the retinotopic site, and within a time window of 100 ms after the local response. In some cases only a local response was observed without the following propagating wave (Figure 4A). In other cases both local and delayed wave were observed, seen in the signal trace from a single detector as double peaks (Figure 4B). In the 15 animals where partial suppression was observed, delayed waves were found in 12 animals.

The delayed propagating wave from a partially suppressed response is different from the local response in several aspects: First, the delayed wave occurred much later (30-80 ms) than the local response. Secondly, the two have different spatiotemporal distributions. As shown in Figure 4, the local response (4A, first peak in gray window of 4B) typically has a higher amplitude at the center (*i2*) and much lower amplitude in surrounding locations (*i1*),

while the delayed propagating wave (4B, second peak in gray window) has similar amplitude at the center (*i2*) and surrounding locations (*i1*).

Local responses and delayed waves can also be distinguished by their initiation sites. As shown in Figure 4, the initiation site of the local response coincides well with the retinotopic site of St2 (Figure 4A, B, images marked by “L”). The initiation sites of the delayed waves, in contrast, were more posterior and medial (Figure 4B image marked by “D”). In this preparation, we have examined 8 trials with delayed waves. In all trials, the initiation sites of the local response were clustered tightly around the retinotopic site of the stimulus, while the initiation sites of the delayed waves scattered over a large area in V1 (Figure 4B right).

These results suggest that visually-evoked responses contain two independent processes, the local response and the subsequent propagating wave. The two can be dissociated when they are weakened by a previous visual stimulus.

Interaction between spontaneous and evoked waves

We next ask whether spontaneous waves of cortical activity can interact with visually-evoked waves, similar to the interaction between two evoked waves. Spontaneous activities observed in cortex at certain anesthetic planes have also been referred to as “UP states” (Steriade et al., 1993; Cowan and Wilson, 1994; Contreras et al., 1996; Petersen et al., 2003b; Sachdev et al., 2004; Rudolph et al., 2007; Okun and Lampl, 2008). In spatiotemporal domains, these spontaneous events manifest as propagating waves (Ferezou et al., 2007; Xu et al., 2007; Han et al., 2008; Huang et al., 2010b). Spontaneous and evoked waves have similar amplitude VSD signals (Figure 5A, traces), but the spontaneous waves often originate outside of the imaging field (Xu et al., 2007). In contrast, the visually-evoked waves we observed were always initiated at or near the retinotopic site (Figure 5A, images).

In our experiments, we gave one visual stimulus in each 3-second recording trial and recorded 100 - 200 trials from each animal. In many trials, spontaneous waves preceded visually-evoked waves at variable intervals. Due to the difficulty of discriminating spontaneous waves following evoked waves, we only examined the interactions between evoked waves and their preceding spontaneous waves.

Figure 5A shows examples in which spontaneous waves suppressed visually-evoked waves. When the spontaneous-to-evoked interval was longer than 300 ms, the evoked activity developed normally from the retinotopic site (Figure 5A traces 1, 5, 6). At shorter intervals, visually-evoked waves were partially or completely suppressed (Figure 5A, traces 2, 3, 4). Group data (Figure 5C) showed obvious amplitude reduction when a spontaneous event preceded the onset of an evoked response by less than 250 ms, similar to the suppression between two visually-evoked waves (Figure 1D). The largest suppression was observed for intervals of 50- 100 ms where visually-evoked responses were completely suppressed in many trials (Figure 5A traces 2).

In some instances, the visually-evoked response occurred nearly simultaneously with a spontaneous event and a fusion of these two activities occurred, resulting in a fused peak in the recording trace (Figure 5B, traces). In the pseudo-color images, the onset of the

spontaneous and evoked waves could be distinguished by their initiation sites (Figure 5B, images). Fusion between a spontaneous and visually-evoked wave (two examples shown in Figure 5B) is similar to that between two visually-evoked waves. Fewer spontaneous-to-evoked fusion cases were seen because the wave-to-wave interval could not be controlled. In the 234 recording trials (n=16 animals) containing spontaneous waves preceding the visually-evoked waves, we observed 9 incidences of fusion. For this reason statistics for ISIs from 0 to 50 ms were omitted in Figure 5C.

Interaction between visually-evoked waves and waves triggered by direct cortical electrical stimulation

In order to examine whether visually-evoked waves can suppress other cortical propagating waves, we delivered electrical shocks to the cortex shortly after the visual stimulus. We first adjusted the visual stimulus so that the retinotopic site on the cortex was approximately 2 mm from the tip of the stimulation electrode (Figure 6A). Electrical stimulation also initiated strong propagating waves, emanating from the tip of the stimulation electrode (Figure 6). We adjusted the intensity of electrical stimulation such that the amplitude of evoked response in the vicinity of the electrode tip was similar to that evoked by the visual stimulus. For Figure 6, the adjusted intensity of the electrical stimulation was approximately 10 μA (0.1 ms square pulse) (Figure 6B middle two traces). When the electrical stimulation intensity was increased to 25 μA, the activation at the stimulation site was larger than that evoked by a visual stimulus (Figure 6B bottom two traces). Visually-evoked waves strongly suppress the activity evoked by a subsequent electrical stimulation. Figure 6C shows an example of the suppression when electrical stimulus was delivered 150 ms after the onset of visual stimulus. At an intensity of 10 μA, the electrically evoked wave was completely suppressed (Figure 6C, top row images). However, when the stimulus intensity was increased, the electric stimulus was still able to induce a propagating wave. In this animal, the propagation of the electrically-evoked response became visible at an intensity of 15 μA (Figure 6C, middle two rows); increasing intensity to 25 μA resulted in an obvious propagating wave (Figure 6C, bottom two rows).

Further analysis showed that the amplitude of the response at the stimulation site was related to the stimulus intensity (Figure 6C, site 2), while the amplitude of response at a distant site was independent of stimulus intensity (Figure 6C, site 1) and was comparable to that of visually evoked responses (Figure 6B). This suggests a propagation mechanism existing within the network, which controls the amplitude of the propagating wave.

To find another reference for the amplitude of the propagating wave, we compared VSD signal amplitude of visually-evoked waves to that of epileptiform spikes (as known as interictal-like spikes) in the same tissue. Epileptiform spikes occur spontaneously after epidural application of bicuculline (1 mM), a drug which blocks GABA-A mediated inhibition. Epileptiform spike is known to have large and stable amplitude in VSD signals (London et al., 1989; Tsau et al., 1998; Ma et al., 2004). At a given condition of VSD staining, illumination and lens numerical aperture, the amplitude of epileptiform spikes in the VSD signals can be used as a relative standard for gauging cortical activation (Takagaki et al. 2008a). We found that in the same tissue the amplitude of spontaneous interictal-like

spikes is about 4-5 times higher than that of visually-evoked waves, suggesting that the cortical neurons have a potential to have much higher level of activity; visually evoked waves only partially active the neuronal population. When two waves fuse, the amplitude of response does not increase, further suggesting that there is a mechanism controlling the level of population activity when multiple visual stimuli are presented.

Discussion

The principal findings of this report are the following: 1) Visually-evoked propagating waves suppressed the wave evoked by a subsequent visual stimulus presented within 80-300 ms. 2) Simultaneous presentation of two visual stimuli at different locations evoked two waves propagating toward each other and fusing in the visual cortex. 3) Fusion did not increase the level of population activity (amplitude of the VSD signal) but significantly shortened the latency and half-width of the response, and resulted in changes in the spatial profile of the wave propagation. 4) The visually-evoked propagating wave was suppressed by the occurrence of a prior spontaneous wave. 5) Electrical stimulus to the cortex can also evoke a propagating wave, which was also suppressed by a prior visually-evoked propagating wave.

These results suggest two properties of propagating waves in visual cortex. First, the propagating waves, both spontaneous and evoked, have a refractory period during which the responses to subsequent visual stimuli are suppressed. Second, the neuronal population within a propagating wave maintains stable but moderate activity, which does not increase when multiple waves meet.

Refractory period

In mammalian visual cortex, both spontaneous and visually-evoked activity can manifest as propagating waves (Xu et al., 2007; Han et al., 2008). Although spontaneous and evoked waves differ in initiation sites and propagation velocity when crossing cortical boundaries (Xu et al., 2007), both can suppress an evoked population response within a defined time window (Figure 1, 5). This timing-dependent suppression (Figure 1D) suggests that there is a refractory period for waves propagating within visual cortex, during which responses to the subsequent stimuli are either reduced or fail to develop (Figure 4). A similar refractory period may also exist in the population activity of other cortical areas. In rodent barrel cortex, a whisker deflection inhibits the population response to subsequent stimuli within an interval of 50 to 200 ms (Civillico and Contreras, 2006). While the barrel cortex is spontaneously depolarized, whisker deflection evokes smaller, briefer and spatially more confined responses (Petersen et al., 2003b). Thus, the refractory period is likely a common feature of propagating waves in sensory cortex. The duration of the refractory period may be slightly different between different cortical areas and different animal species. In rodent visual cortex, the refractory period of the propagating wave was about 300 ms. Our results also suggest that the refractory period is relative. During the refractory period, while other visual stimuli can not evoke new waves, a strong electrical stimulus can simultaneously activate more neurons in the population and initiate another propagating wave (Figure 6C).

Local response and delayed propagating wave

Results in Figure 4 suggest that visually-evoked cortical activity contains two independent processes. One is the local response occurring only at the cortical retinotopic representation site and the other is a propagating wave affecting large areas. The local response is likely to be directly evoked by thalamic afferents to the cortex, has a fixed location in the cortex affecting a relatively fixed population of neurons receiving thalamic input. The waves, in contrast, do not have a fixed initiation site (Figure 4B), suggesting polysynaptic interactions (e.g., excitatory feedback from higher visual areas, corticothalamic loops and other subcortical polysynaptic interactions). The local response and the subsequent propagating wave cannot be distinguished when a single visual stimulus is given, in which the local response is masked by promptly developed propagating wave. When the second visual stimulus (St2) is given during the refractory period of the response to St1 (Figure 4B), the development of the St2-evoked propagating wave is largely suppressed, which unmasks the local response.

Sustaining of a wave and amplitude control

Previous studies have shown that in propagating waves, individual neurons mildly depolarize (Petersen et al., 2003b; Poulet and Petersen, 2008). Such small depolarizations can slightly increase the firing probability of a neuron (Steriade et al., 2001; Shu et al., 2003; Steriade and Timofeev, 2003). In cortical layer II-III, neurons are extensively interconnected (Levitt and Lund, 2002; Douglas and Martin, 2004; Thomson and Lamy, 2007; Voges et al., 2010) and one spike can evoke excitatory post-synaptic potentials (EPSPs) in thousands of its post-synaptic neurons. In this way, a small number of spikes should be able to maintain a low level of depolarization across the whole network. This depolarization will increase the firing probability of the population and in turn generate more spikes. Statistically, if at time t0 the spikes in a population can generate the same number of spikes later at time t1, the depolarization will be stable and sustained. However, such mild population depolarization cannot be stably sustained without propagation, as explained below.

Depolarized neurons reduce their firing probability by a variety of adaptation mechanisms such as voltage-gated and calcium-dependent potassium conductances, inactivation of low threshold calcium channels, and de-activation of the H current (Borg-Graham et al., 1998; McCormick, 2004). In addition, the activation of principal neurons may activate inhibitory circuits that hyperpolarize principal neurons and decrease their likelihood of spiking (Trevelyan et al., 2006). Therefore, the capability for spike generation in a population would decrease after a wave front passes, resulting in the refractory tail of the wave. The propagating wave is an effective way to prolonging sensory evoked activity in the cortex, by recruiting new and more excitable neurons from the wave front and releasing less excitable neurons in the tail of the wave.

We observed that the amplitude of the electrically-evoked response is independent of the stimulus intensity at locations distant from the initiation site, suggesting that the amplitude of the wave may be controlled by internal cortical circuit mechanisms (Figure 6B site 1). Local inhibitory circuits may play a major regulatory role in controlling the level of population depolarization. Spiking of the principal neurons in the wave may activate

inhibitory neurons that diffusely shunt and hyperpolarize surrounding neurons to limit the population depolarization. It is well known that when local inhibitory circuits are impaired, the amplitude of the population activation significantly increases (London et al., 1989; Ma et al., 2004; Lippert et al., 2007). The existence of such a mechanism may explain why the interaction of two waves does not increase the amplitude. If one wave already activates the population to the level allowed by internal mechanisms, fusing with another wave cannot further depolarize the population, consistent with the finding that no noticeable increase was observed in the VSD signal (Figures 1D, 2E). However, fusion between two waves can accelerate the time course of population depolarization, resulting in a reduced latency and half-width at the fusion area (Figure 2C).

Propagation observed in this report is a sequential activation in space and time, is likely to be carried out in two-dimensional cortical networks with non-specific (distributed) connections. While local horizontal connections in cortical layers II-III provide sufficient excitable networks for propagation and wave interactions, long-range and subcortical mechanisms may also contribute (Ermentrout and Kleinfeld 2001). For example, abrupt change in propagating velocity (wave “compression”) may be attributed to inhibitions from a remote area via callosal fibers (Xu et al., 2007).

Possible functions

The sensory-evoked wave may be related to perception of novel stimulus. The propagating wave is generated only at the onset of the stimulus, suggesting that the wave is related to the new or a significant change in stimulus parameters. Characteristics of visually-evoked waves depend on the retinotopic site of the stimulus, but do not vary with the shape, duration and orientation of the stimulus (Xu et al., 2007), sharing the characteristics of exogenous attention (Kinchla, 1992; Egeth and Yantis, 1997; Busse and Katzner, 2006). More generally, a single whisker deflection or a small dot visual stimulus can evoke propagating waves over a large area, including the primary sensory and other cortical areas (Petersen et al., 2003a; Jancke et al., 2004b; Civillico and Contreras, 2006; Ferezou et al., 2006; Roland et al., 2006; Ferezou et al., 2007; Xu et al., 2007; Frostig et al., 2008; Takagaki et al., 2008b), suggesting that the wave is not only correlated to specific whiskers or to a specific location in the visual field. Instead, a sensory-evoked propagating wave can increase the neuronal firing probability and synaptic transmission efficacy in a large area which may alter the cortical gain and background activity to prepare for it for incoming stimulus, increasing its sensitivity to fine detail (Treue, 2001; Pessoa et al., 2003; Reynolds and Chelazzi, 2004). The refractory period of the propagating wave may contribute to the processes of pre-pulse inhibition during which the first and weaker stimulus can suppress an animal’s startle response to a subsequent stimulus (Hoffman and Searle, 1965; Hoffman and Ison, 1980).

Propagating direction and velocity determine when and where the cortical network is modified by the sensory activation. The wave front may make a large impact on local excitability. Neurons may have higher excitability to synaptic inputs when a wave front is approaching and the excitability would drop sharply after the wave front sweeps through the area. These changes would happen on a fast time scale of ~10 ms. Although we did not

provide direct evidence at the intracellular level, changes in excitability are likely used to synchronize activity and spike-timing dependent plasticity. Thus, propagating waves are like an organizer; those neurons at the wave front are likely to fire synchronously. The change in wave front caused by the wave fusion would change the organization of firing in different neurons, may play important role in sensory processes, such as apparent motion (Jancke et al., 2004a; Ahmed et al., 2008).

In conclusion, sensory-evoked propagating waves are a widely-observed phenomena in the surface layers of cortex in most sensory modalities studied to date. A propagating wave can mildly activate a vast population of neurons not directly receiving thalamus afferent of the stimulus. The interaction between two evoked waves may contribute to sensory processing by modifying the spatiotemporal profile of population neuronal activity evoked by sensory events.

Acknowledgments

Supported by NIH grant NS059034 (JYW), National Basic Research Program of China (Grant No. 2005CB724301), National High Technology Research and Development Program of China (Grant No. 2007AA02Z313), National Natural Science Foundation of China (Grant No. 90408020) (BL), Humboldt Stiftung/ Foundation (KT).

References

Ahmed B, Hanazawa A, Undeman C, Eriksson D, Valentiniene S, Roland PE. Cortical dynamics subserving visual apparent motion. Cereb Cortex. 2008; 18:2796–2810. [PubMed: 18375528]

Benucci A, Frazor RA, Carandini M. Standing waves and traveling waves distinguish two circuits in visual cortex. Neuron. 2007; 55:103–117. [PubMed: 17610820]

Borg-Graham LJ, Monier C, Fregnac Y. Visual input evokes transient and strong shunting inhibition in visual cortical neurons. Nature. 1998; 393:369–373. [PubMed: 9620800]

Bringuier V, Chavane F, Glaeser L, Fregnac Y. Horizontal propagation of visual activity in the synaptic integration field of area 17 neurons. Science. 1999; 283:695–699. [PubMed: 9924031]

Busse L, Katzner S. The time course of shifting visual attention. J Neurosci. 2006; 26:3885–3886. [PubMed: 16611802]

Civillico EF, Contreras D. Integration of evoked responses in supragranular cortex studied with optical recordings in vivo. J Neurophysiol. 2006; 96:336–351. [PubMed: 16571736]

Contreras D, Timofeev I, Steriade M. Mechanisms of long-lasting hyperpolarizations underlying slow sleep oscillations in cat corticothalamic networks. J Physiol. 1996; 494(Pt 1):251–264. [PubMed: 8814619]

Cowan RL, Wilson CJ. Spontaneous firing patterns and axonal projections of single corticostriatal neurons in the rat medial agranular cortex. J Neurophysiol. 1994; 71:17–32. [PubMed: 8158226]

Douglas RJ, Martin KA. Neuronal circuits of the neocortex. Annu Rev Neurosci. 2004; 27:419–451. [PubMed: 15217339]

Egeth HE, Yantis S. Visual attention: control, representation, and time course. Annu Rev Psychol. 1997; 48:269–297. [PubMed: 9046562]

Ermentrout GB, Kleinfeld D. Traveling electrical waves in cortex: insights from phase dynamics and speculation on a computational role. Neuron. 2001; 29:33–44. [PubMed: 11182079]

Ferezou I, Bolea S, Petersen CC. Visualizing the cortical representation of whisker touch: voltage-sensitive dye imaging in freely moving mice. Neuron. 2006; 50:617–629. [PubMed: 16701211]

Ferezou I, Haiss F, Gentet LJ, Aronoff R, Weber B, Petersen CC. Spatiotemporal dynamics of cortical sensorimotor integration in behaving mice. Neuron. 2007; 56:907–923. [PubMed: 18054865]

Frostig RD, Xiong Y, Chen-Bee CH, Kvasnak E, Stehberg J. Large-scale organization of rat sensorimotor cortex based on a motif of large activation spreads. J Neurosci. 2008; 28:13274–13284. [PubMed: 19052219]

Grinvald A, Hildesheim R. VSDI: a new era in functional imaging of cortical dynamics. Nat Rev Neurosci. 2004; 5:874–885. [PubMed: 15496865]

Grinvald A, Hildesheim R, Farber IC, Anglister L. Improved fluorescent probes for the measurement of rapid changes in membrane potential. Biophys J. 1982; 39:301–308. [PubMed: 7139029]

Han F, Caporale N, Dan Y. Reverberation of recent visual experience in spontaneous cortical waves. Neuron. 2008; 60:321–327. [PubMed: 18957223]

Hoffman HS, Ison JR. Reflex modification in the domain of startle: I. Some empirical findings and their implications for how the nervous system processes sensory input. Psychol Rev. 1980; 87:175–189. [PubMed: 7375610]

Hoffman HS, Searle JL. Acoustic Variables in the Modification of Startle Reaction in the Rat. J Comp Physiol Psychol. 1965; 60:53–58. [PubMed: 14334243]

Huang X, Troy WC, Yang Q, Ma H, Laing CR, Schiff SJ, Wu JY. Spiral waves in disinhibited mammalian neocortex. J Neurosci. 2004; 24:9897–9902. [PubMed: 15525774]

Huang, X.; Xu, W.; Jin, W.; Wu, JY. Monitoring population membrane potential signals from neocortex. In: Canepari, M.; Zecevic, D., editors. The Voltage Imaging Book. Springer Press; 2010a. p. 71-81.

Huang X, Xu W, Liang J, Takagaki K, Gao X, Wu JY. Spiral wave dynamics in neocortex. Neuron. 2010b; 68:978–990. [PubMed: 21145009]

Jancke D, Chavane F, Naaman S, Grinvald A. Imaging cortical correlates of illusion in early visual cortex. Nature. 2004a; 428:423–426. [PubMed: 15042090]

Jancke D, Erlhagen W, Schoner G, Dinse HR. Shorter latencies for motion trajectories than for flashes in population responses of cat primary visual cortex. J Physiol. 2004b; 556:971–982. [PubMed: 14978201]

Jin W, Zhang RJ, Wu JY. Voltage-sensitive dye imaging of population neuronal activity in cortical tissue. J Neurosci Methods. 2002; 115:13–27. [PubMed: 11897360]

Kinchla RA. Attention. Annu Rev Psychol. 1992; 43:711–742. [PubMed: 1539951]

Levitt JB, Lund JS. The spatial extent over which neurons in macaque striate cortex pool visual signals. Vis Neurosci. 2002; 19:439–452. [PubMed: 12511077]

Lippert MT, Takagaki K, Xu W, Huang X, Wu JY. Methods for voltage-sensitive dye imaging of rat cortical activity with high signal-to-noise ratio. J Neurophysiol. 2007; 98:502–512. [PubMed: 17493915]

London JA, Cohen LB, Wu JY. Optical recordings of the cortical response to whisker stimulation before and after the addition of an epileptogenic agent. J Neurosci. 1989; 9:2182–2190. [PubMed: 2723769]

Ma HT, Wu CH, Wu JY. Initiation of spontaneous epileptiform events in the rat neocortex in vivo. J Neurophysiol. 2004; 91:934–945. [PubMed: 14534285]

McCormick, DA. Membrane properties and neurotransmitter actions. In: Shepherd, GM., editor. The Synaptic Organization of the Brain. New York: Oxford University Press; 2004. p. 39-77.

Okun M, Lampl I. Instantaneous correlation of excitation and inhibition during ongoing and sensory-evoked activities. Nat Neurosci. 2008; 11:535–537. [PubMed: 18376400]

Pessoa L, Kastner S, Ungerleider LG. Neuroimaging studies of attention: from modulation of sensory processing to top-down control. J Neurosci. 2003; 23:3990–3998. [PubMed: 12764083]

Petersen CC, Grinvald A, Sakmann B. Spatiotemporal dynamics of sensory responses in layer 2/3 of rat barrel cortex measured in vivo by voltage-sensitive dye imaging combined with whole-cell voltage recordings and neuron reconstructions. J Neurosci. 2003a; 23:1298–1309. [PubMed: 12598618]

Petersen CC, Hahn TT, Mehta M, Grinvald A, Sakmann B. Interaction of sensory responses with spontaneous depolarization in layer 2/3 barrel cortex. Proc Natl Acad Sci U S A. 2003b; 100:13638–13643. [PubMed: 14595013]

Poulet JF, Petersen CC. Internal brain state regulates membrane potential synchrony in barrel cortex of behaving mice. Nature. 2008; 454:881–885. [PubMed: 18633351]

Prechtl JC, Bullock TH, Kleinfeld D. Direct evidence for local oscillatory current sources and intracortical phase gradients in turtle visual cortex. Proc Natl Acad Sci U S A. 2000; 97:877–882. [PubMed: 10639173]

Prechtl JC, Cohen LB, Pesaran B, Mitra PP, Kleinfeld D. Visual stimuli induce waves of electrical activity in turtle cortex. Proc Natl Acad Sci U S A. 1997; 94:7621–7626. [PubMed: 9207142]

Reynolds JH, Chelazzi L. Attentional modulation of visual processing. Annu Rev Neurosci. 2004; 27:611–647. [PubMed: 15217345]

Roland PE, Hanazawa A, Undeman C, Eriksson D, Tompa T, Nakamura H, Valentiniene S, Ahmed B. Cortical feedback depolarization waves: A mechanism of top-down influence on early visual areas. Proc Natl Acad Sci U S A. 2006; 103:12586–12591. [PubMed: 16891418]

Rudolph M, Pospischil M, Timofeev I, Destexhe A. Inhibition determines membrane potential dynamics and controls action potential generation in awake and sleeping cat cortex. J Neurosci. 2007; 27:5280–5290. [PubMed: 17507551]

Sachdev RN, Ebner FF, Wilson CJ. Effect of subthreshold up and down states on the whisker-evoked response in somatosensory cortex. J Neurophysiol. 2004; 92:3511–3521. [PubMed: 15254074]

Schiff SJ, Huang X, Wu JY. Dynamical evolution of spatiotemporal patterns in mammalian middle cortex. Phys Rev Lett. 2007; 98:178102. [PubMed: 17501537]

Senseman DM, Robbins KA. Modal behavior of cortical neural networks during visual processing. J Neurosci. 1999; 19:RC3. [PubMed: 10234049]

Sharon D, Jancke D, Chavane F, Na'aman S, Grinvald A. Cortical response field dynamics in cat visual cortex. Cereb Cortex. 2007; 17:2866–2877. [PubMed: 17395608]

Shu Y, Hasenstaub A, McCormick DA. Turning on and off recurrent balanced cortical activity. Nature. 2003; 423:288–293. [PubMed: 12748642]

Song WJ, Kawaguchi H, Totoki S, Inoue Y, Katura T, Maeda S, Inagaki S, Shirasawa H, Nishimura M. Cortical intrinsic circuits can support activity propagation through an isofrequency strip of the guinea pig primary auditory cortex. Cereb Cortex. 2006; 16:718–729. [PubMed: 16107586]

Steriade M, Nunez A, Amzica F. A novel slow (< 1 Hz) oscillation of neocortical neurons in vivo: depolarizing and hyperpolarizing components. J Neurosci. 1993; 13:3252–3265. [PubMed: 8340806]

Steriade M, Timofeev I. Neuronal plasticity in thalamocortical networks during sleep and waking oscillations. Neuron. 2003; 37:563–576. [PubMed: 12597855]

Steriade M, Timofeev I, Grenier F. Natural waking and sleep states: a view from inside neocortical neurons. J Neurophysiol. 2001; 85:1969–1985. [PubMed: 11353014]

Takagaki K, Lippert MT, Dann B, Wanger T, Ohl FW. Normalization of voltage-sensitive dye signal with functional activity measures. PLoS One. 2008a; 3:e4041. [PubMed: 19116673]

Takagaki K, Zhang C, Wu JY, Lippert MT. Crossmodal propagation of sensory-evoked and spontaneous activity in the rat neocortex. Neurosci Lett. 2008b; 431:191–196. [PubMed: 18178313]

Thomson AM, Lamy C. Functional maps of neocortical local circuitry. Front Neurosci. 2007; 1:19–42. [PubMed: 18982117]

Treue S. Neural correlates of attention in primate visual cortex. Trends Neurosci. 2001; 24:295–300. [PubMed: 11311383]

Trevelyan AJ, Sussillo D, Watson BO, Yuste R. Modular propagation of epileptiform activity: evidence for an inhibitory veto in neocortex. J Neurosci. 2006; 26:12447–12455. [PubMed: 17135406]

Tsau Y, Guan L, Wu JY. Initiation of spontaneous epileptiform activity in the neocortical slice. J Neurophysiol. 1998; 80:978–982. [PubMed: 9705483]

Voges N, Schuz A, Aertsen A, Rotter S. A modeler's view on the spatial structure of intrinsic horizontal connectivity in the neocortex. Prog Neurobiol. 2010; 92:277–292. [PubMed: 20685378]

Wang XJ. Neurophysiological and computational principles of cortical rhythms in cognition. Physiol Rev. 2010; 90:1195–1268. [PubMed: 20664082]

Wu, JY.; Cohen, LB. Fast multisite optical measurement of membrane potential. In: Mason, WT., editor. Biological Techniques: Fluorescent and Luminescent Probes for Biological Activity. New York: Academic Press; 1993. p. 389-404.

Wu JY, Xiaoying H, Chuan Z. Propagating waves of activity in the neocortex: what they are, what they do. Neuroscientist. 2008; 14:487–502. [PubMed: 18997124]

Xu W, Huang X, Takagaki K, Wu JY. Compression and reflection of visually evoked cortical waves. Neuron. 2007; 55:119–129. [PubMed: 17610821]

Abbreviations

VSD	voltage-sensitive dye
ISI	inter-stimulus interval
V1	primary visual cortex
V2	secondary visual cortex
GABA	gamma-Aminobutyric acid

Highlights

- Visually-evoked cortical waves were examined with voltage-sensitive dye imaging.
- Evoked waves suppressed subsequent evoked waves during a window of 80-300 ms.
- Simultaneously evoked waves propagated toward each other and fused.
- Fusion significantly changed the spatiotemporal profile of propagation.
- Occurrence of spontaneous waves suppressed visually-evoked waves.

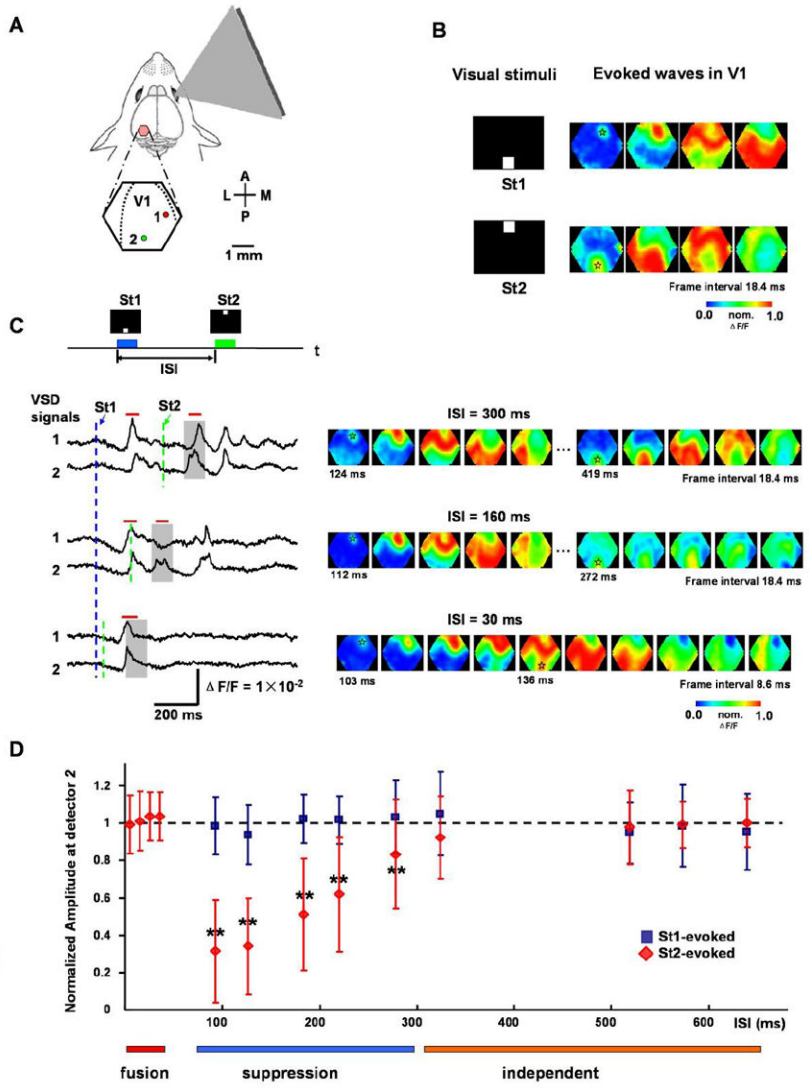

Figure 1. Interactions between visually-evoked waves

(A) Schematic drawing of experimental arrangement. The visual stimuli are bright squares (duration = 100 ms, 10 × 10 degrees visual angle), presented on a CRT screen to the right eye. A cranial window (5 mm in diameter) over the left visual cortex was centered over the primary visual area (V1). The hexagon outlines the imaging field (approximately 4 mm in diameter) and dashed lines mark the borders between V1 and V2. A: anterior, P: posterior, M: medial, L: lateral. Two detectors, 1 and 2, are selected from a total of 464 detectors, where 2 is near the retinotopic site of St2 and 1 is at a mid-medial location between the retinotopic sites of St1 and St2. Their signal traces are shown in (C). The pseudo-color images in B and C are 0.6-ms snap shot selected from a total of 5120 frames in a 3-second trial. The VSD signal on each detector is normalized to its own peak and converted to pseudo-color images according to a color scale (middle) after a 3-30 Hz temporal filtering and a 3 × 3 mean spatial filtering.

(B) ***Left:*** Visual stimuli displayed at the bottom (St1) or top (St2) of the screen. ***Right:*** Pseudo-color images of the response evoked by St1 or St2. The transparent asterisks mark the retinotopic site of St1 or St2.
(C) Interactions of responses evoked by two sequential visual stimuli. ***Top:*** Two squares St1 and St2, separated by 45 degrees of visual angle in the visual field, are displayed sequentially with a given inter-stimulus interval (ISI) (blue and green bars). ***Bottom: Left***: Sample traces of optical signals (filtered by 3-200 Hz and heartbeat artifact removed) from detectors 1 and 2 (locations shown in A). The dashed lines mark the onset times of the stimuli (blue for St1 and green for St2). The gray shades indicate the time window for expected occurrence of St2 responses. Note that the response to St2 is reduced at ISI=160ms and fused into one peak with first response at ISI=30ms. Red bars on top of the traces mark the durations of the images on the right. ***Right:*** The pseudo-color images of the signals during the time period indicated by the red bars on the left. The time below images mark the timing (from the St1 onset) of the frames, in which the initiation sites are visible. The transparent asterisks mark the initial sites of the evoked waves. Note that at ISI = 30 ms, the second wave initiated before the arrival of the first wave and fused with the first wave.
(D) Amplitude reduction of the second wave. Data were collected from 1011 trials (16 animals). The amplitude was measured at the retinotopic site of St2 (e.g. detector 2 in A) and was normalized to that evoked by single stimulus in the same animal. Cross-animal averaging was done after the normalization. Blue squares are for the responses evoked by the first stimulus (St1) and red diamonds are for the responses evoked by the second stimulus (St2). T-test was done at each testpoint (the control is the amplitude of the wave evoked by a single stimulus St2) and those with significant difference were marked by "**" ($p < 0.01$). Color bars under the plot mark the time window for different types of interactions.

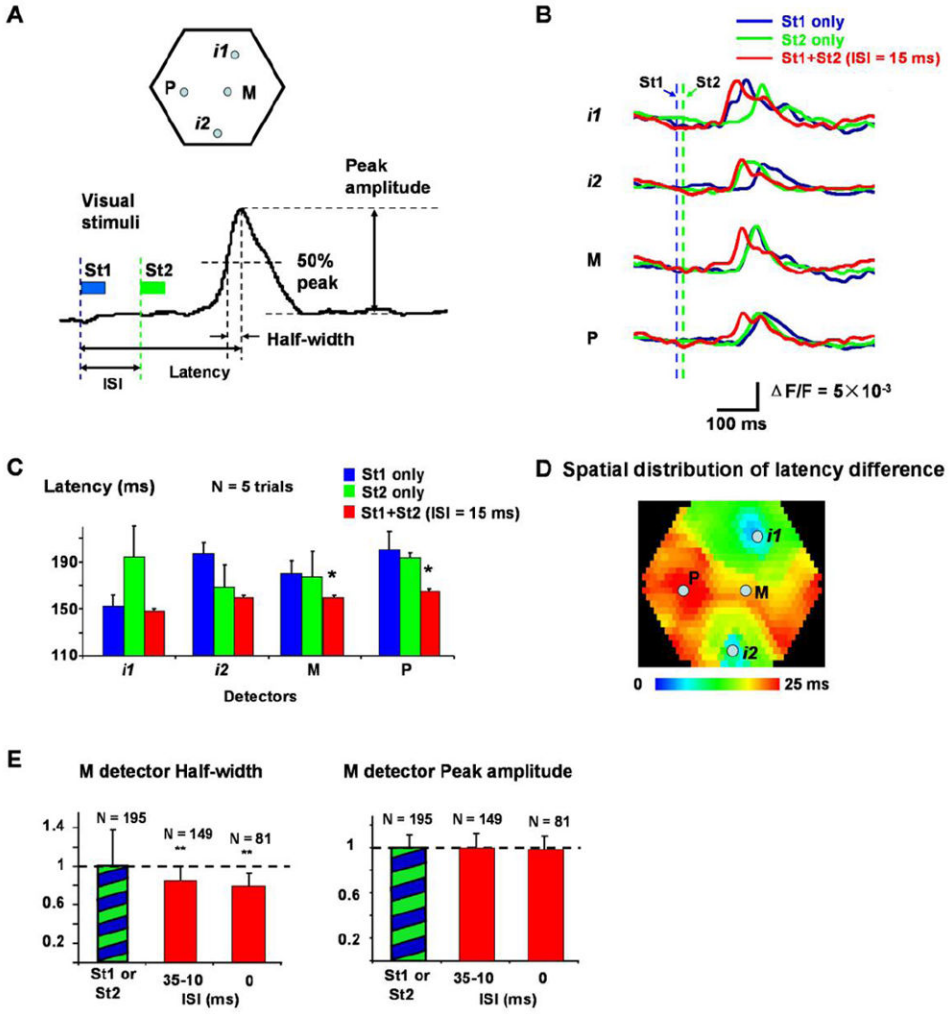

Figure 2. Latency and half-width are shortened by wave fusion

(A) ***Top***: Locations of the four detectors, *i1*, *i2*, M and P used in (B-E). *i1* and *i2* are approximately at the retinotopic sites of St1 and St2; M is at the center of the line from *i1* to *i2*, and P is about 1.5 mm lateral to M. ***Bottom***: Definitions of ISI, latency, half-width and peak amplitude. Blue and green bars indicate the duration of the St1 and St2. Blue and green dashed lines mark the onset time of the two visual stimuli.

(B) Latency shortening seen in optical signals (single trial filtered by 1.5 - 30 Hz). Signals from four detectors, *i1*, *i2*, P and M are shown. Traces from three stimulation conditions are superimposed: St1 alone (blue), St2 alone (green), and St1 preceding St2 with 15 ms ISI (red). Blue and green dashed lines mark the onset time of St1 and St2.

(C) Latency shortening of 5 trials averaging. Latency at detectors M and P was significantly shortened when ISI = 15ms (marked by "*", compare to both blue and green bars in the same group, t-test, $p < 0.05$). Data in C and B are from the same experiment.

(D) Spatial distribution of latency changes at ISI = 15 ms (averaged from 5 trials as in C). The color indicates the latency changes at each location, from no change (blue) to shortened 25 ms (red). The control latency on each detector is the lesser of the latency of St1 or St2

evoked response. Note that around retinotopic sites, the latency shows little changes (blue-green) while large changes occur in the middle areas between the two retinotopic sites. (E) Changes in the half-width and peak amplitude. The signals at detector M were analyzed. ***Left:*** The half-width of the response at different ISIs (averaged from 6 animals). Columns marked by "**" are significantly different (t-test, $p < 0.01$) from the control (green-blue bar). ***Right:*** Peak amplitude of the response at different ISIs (averaged from 6 animals, cross-animal averaging was done after the normalization, same as Figure 1D). N is the number of averaged trials.

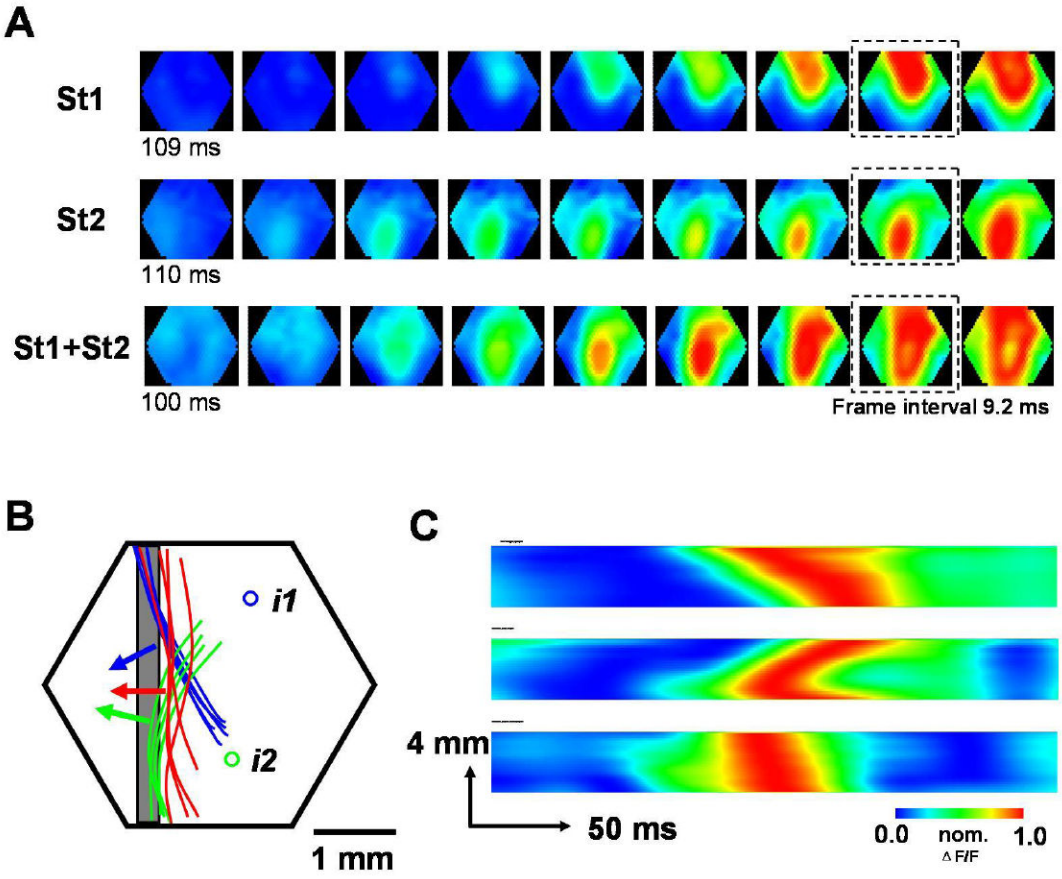

Figure 3. Wave front changed by wave fusion

(A) Sequential snap shots (inter-frame interval 9.2 ms) of the evoked waves under three stimulus paradigms: St1 alone (top row), St2 alone (middle row), St1 and St2 simultaneously (bottom row). The broken squares mark the frames from which the contour of wave front was drawn in B. The contour line was traced along the border between yellow and red color in pseudo color image (about 70% of peak). For clarity of the presentation, only the left part of the contour was used in B.

(B) Hexagon indicates the imaging field. *i1* and *i2* are the retinotopic sites of St1 and St2. Blue, green and red curves are wave front contour lines drawn from the frames (marked by broken squares in A) ~50 ms after when the initiation site become visible in the image. The blue curves are from 5 trails (St1 alone) and the green curves are from 4 trails (St2 alone), while the red curves are from 4 trails (St1 and St2 simultaneously). The arrows show the approximate direction vectors of the waves that are perpendicular to the wave front. The gray box indicates the column of detectors used to make the X-T map in C.

(C) Space-time maps (X-T maps) under three stimulus paradigms: St1 alone (top), St2 alone (middle), St1 and St2 simultaneously (bottom). The X-T maps were made from the signals in a column of detectors (marked by gray box in B). Note that when two visual stimuli are given simultaneously, the depolarization along the detector column reach the peak almost simultaneously (bottom image), markedly different from when individual visual stimulus is given alone (top two images).

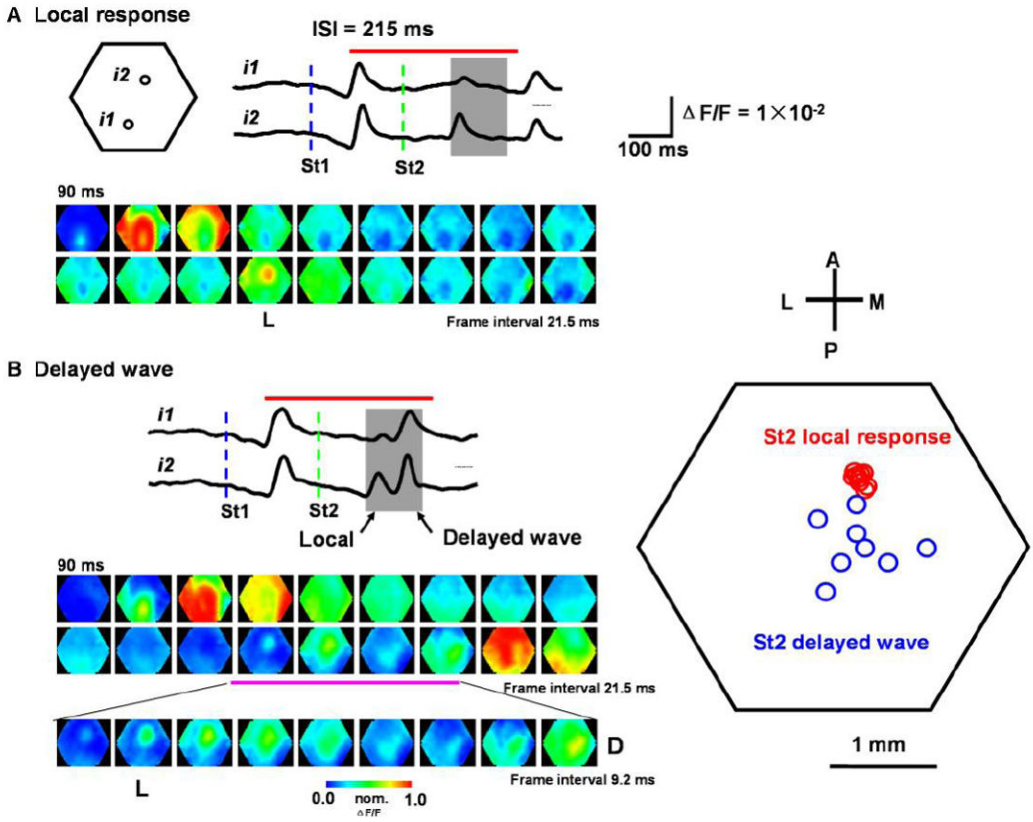

Figure 4. Suppression of the second wave

(A) Local response evoked by the second stimulus. ***Top:*** Traces from the detectors *i1* and *i2* (filtered by 3-30 Hz). Blue and green dashed lines mark the onset time of the two stimuli. Gray shade indicates the time window for the expected occurrence of the second response. Red bar on the top of traces indicates the time window for the images at the bottom. ***Bottom:*** Pseudo-color images within the period marked by the red bar. Note that the response to St1 developed into a propagating wave, while the response to St2 is suppressed, with only a local response (image marked by "L").

(B) Delayed wave evoked by the second stimulus. ***Left:*** Traces and images are from another trial of the same experiment. The second response (in the gray shade) showed two peaks. The first peak is much larger at *i2* than at *i1*, corresponding to the local response seen in the bottom images (L). The second peak is seen in both *i1* and *i2* and the images indicate it is a propagating wave. The red bar on the top of the traces indicates the time window for the images in two upper rows. The third row of images is an expansion of part of the second row (marked by pink bar). Frames marked by "L" and "D" show the initiation sites of the local response and delayed wave respectively. ***Right:*** Initiation sites of local response and delayed waves from 8 trials of the same animal. Note that the initiation sites of the local response (red circles) are clustered around *i2*, while the initiation sites of the delayed wave (blue circles) are scattered in a larger area.

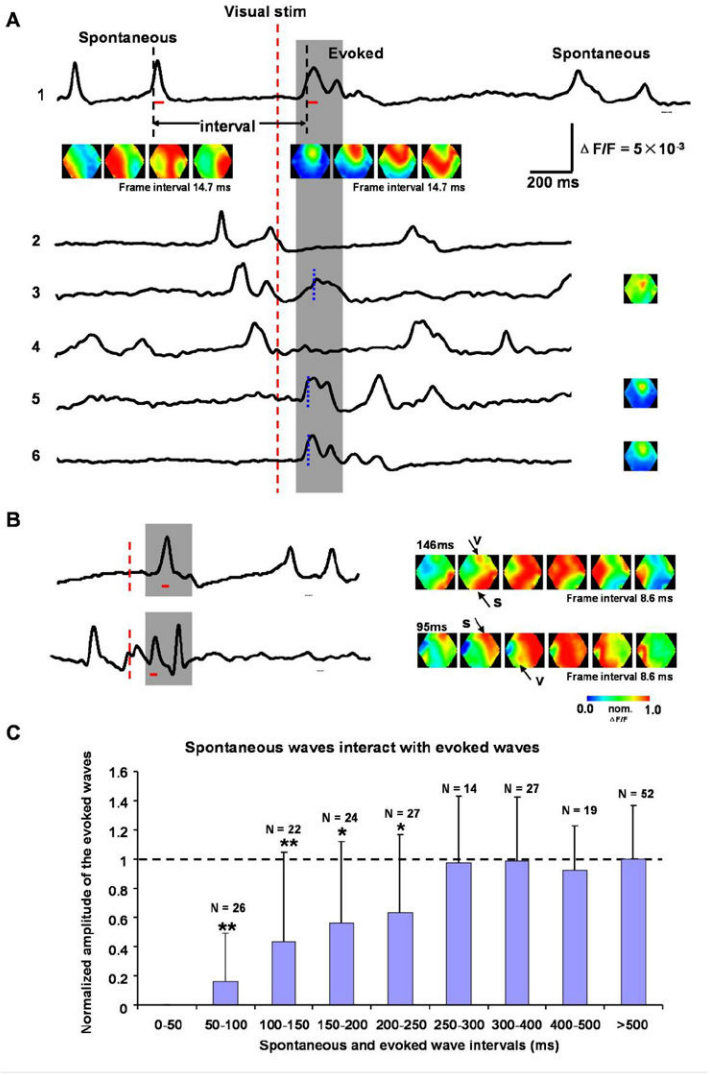

Figure 5. Interactions between spontaneous and visually-evoked waves

(A) Examples for interactions between spontaneous and evoked waves. The traces are from the retinotopic site and from different trials in the same experiment. The red dashed line marks the onset of the visual stimulus. Two black dashed lines mark the half-peak time of the evoked and the nearest preceding spontaneous wave. The interval between spontaneous and evoked waves is defined as the time between these two black dashed lines. Gray shade shows the time window for the expected visual response. The red bars under the top trace mark the time window for the images below. Images below trace 1 show a spontaneous (left row) and an evoked wave (right row). The images on the right of traces 3, 5 and 6 show the initiation sites of the evoked responses. The timing for each image is marked by the blue broken lines on each trace. Scale bars are for traces in both A and B.

(B) Examples of fusion between spontaneous and evoked waves. ***Left:*** Optical traces from the retinotopic sites. Red dashed lines mark the onset of the visual stimulus and the gray shade indicates the time window for the expected response. The red bars under the traces mark the time window for the images on the right. ***Right:*** The pseudo-color images of the

signals during the period indicated by the red bars on the left. Arrows show the spontaneous (s) and evoked waves (v). The two examples are from different animals.

(C) Spontaneous waves suppress subsequent evoked waves. The amplitudes of the evoked response are measured at the retinotopic site in each animal and normalized to that of the response when no spontaneous activity occurred during 1000 ms before visual stimulus. The intervals are defined as in (A). The columns marked by "*" are statistically different (t-test, $p < 0.05$) and those marked by "**" are significant different ($p < 0.01$) from the control (horizontal dashed line). The evoked responses are suppressed at intervals of 50-250 ms. For intervals longer than 250 ms, the response amplitudes show no obvious change. Data are from 16 animals and N indicates the number of trials for averaging.

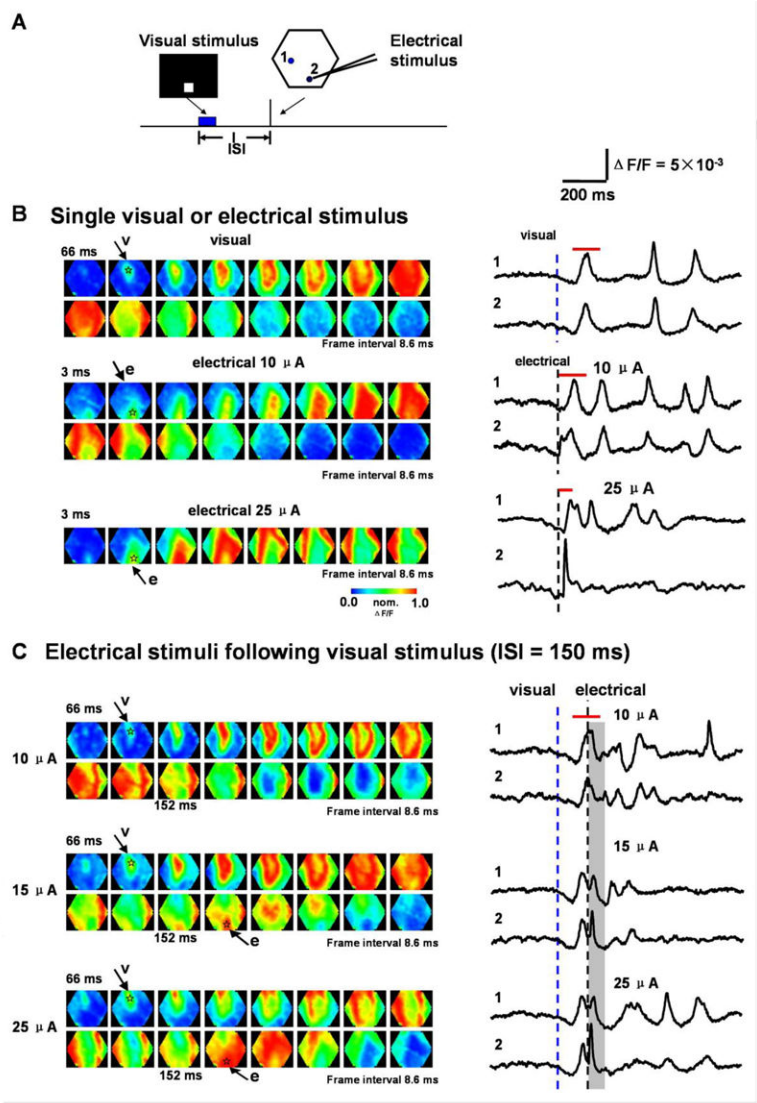

Figure 6. Interaction between visually and electrically evoked waves

(A) Experimental arrangement. The hexagon outlines the imaging field. 1 and 2 mark the detectors used in B and C. Detector 2 is near the site of the electrical stimulus. The ISI is defined as the time between the onset of visual and electrical stimulus (Blue box marks the duration of visual stimulus; black bar marks the electrical stimulus).

(B) ***Left:*** Images of waves evoked by visual or electrical stimuli: Visual stimulus only (top 2 rows); Electrical stimulus only (middle 2 rows, 10 μA ; bottom 2 rows, 25 μA). Arrows mark the frames in which the initiation of the visually (v) or electrically (e) evoked waves are visible. The transparent asterisks mark the initiation sites. ***Right:*** Traces from detector 1 and 2 (location marked in A, filtered between 3-200 Hz after 3×3 spatial filtered). Blue or black dashed lines show the onset of the visual or electrical stimulus, respectively. The red bars above each trace mark the time window for the images on the left.

(C) Interaction between visually and electrically evoked waves. The visual stimulus is followed by an electrical stimulation with different intensity at an ISI of 150 ms. ***Left:***

Pseudo-color images for the responses from the same preparation as in B. Arrows mark the frames where the initiation of the visually (v) or electrically (e) evoked waves are visible. The transparent asterisks mark the initiation sites. ***Right:*** Traces from detectors 1 and 2 (location marked in A, filtered between 3-200 Hz after 3×3 spatial filtering). Blue and black dashed lines denote the onset of the visual and electrical stimulus respectively. Gray shade indicates the period for the expected electrical evoked response. The red bars above the traces mark the time window for the images on the left.